Design of GaAs nanowires array based photovoltaic solar cells: simulations of optical reflectance

R M de la Cruz[a,1,*], C Kanyinda-Malu[b], J E Muñoz Santiuste[c]

[a] *Departamento de Física, Universidad Carlos III de Madrid, EPS. Avda. de la Universidad 30, 28911 Leganés (Madrid), Spain*
[b] *Departamento de Economía Financiera y Contabilidad II, Area de Matemáticas y Estadística, Universidad Rey Juan Carlos, FCJS, Paseo de los Artilleros s/n, 28032 Madrid, Spain*
[c] *Departamento de Física, Universidad Carlos III de Madrid, EPS. Avda. de la Universidad 30, 28911 Leganés (Madrid), Spain*

Abstract

We report the optical response of a periodic square array of GaAs nanowires embedded in epoxy as a candidate for photovoltaic solar cells. The simulated system is a multilayer array constituted by alternating layers of epoxy and an effective medium constituted by GaAs nanowires arrays embedded in epoxy. To discuss the optical response, we investigate the reflectance dependence on the number of bilayers considered in the array and the angle of incident light. The GaAs nanowire dielectric function is described in terms of Webb formalism to take into account the confinement energy of the excitons. The effective dielectric function of GaAs nanowires embedded in epoxy is evaluated within the Maxwell–Garnett theory. We evaluate the reflectance for s- and p-polarized light through the transfer matrix formalism for n bilayers. For both s- and p-polarization, we observe an oscillating behavior of the reflectance, similar to that reported in the literature. We have also obtained a feature peaked around 850 nm. While the oscillations can be ascribed to multiple interference from periodic bilayers, the peak at 850 nm can be understood in term of the gap energy in the nanowire dielectric function.

*Corresponding author
Email addresses: rmc@fis.uc3m.es (R M de la Cruz), clement.kanyindamalu@urjc.es (C Kanyinda-Malu), jems@fis.uc3m.es (J E Muñoz Santiuste)
[1]Phone: +34 91 624 8733,Fax: +34 91 624 8749

Attending to the reflectance dependence on the light incidence angle, we have found that for s-polarized light, the reflectance is higher with increasing angles, in comparison to p-polarized light cases.

Keywords:
GaAs nanowires array, Reflectance, Transfer matrix formalism,
Maxwell–Garnett effective model, Solar cells
PACS: 78.20. Bh, 78.20.Ci, 78.55.Cr, 78.67.-n

1. Introduction

For the last decades, there is a great interest in the research of photovoltaic solar cells as it is demonstrated by an increasing literature on this field. The photovoltaic solar energy, sustainable and renewable source, could be one of the alternatives to the traditional designs based on fossil fuels energy [1, 2]. For this purpose, the increase of the solar cell power conversion efficiency (PCE) is essential in order to reduce all costs scaling with system size [3, 4]. Nowadays, the solar cells are mainly based on planar single junction, limited in PCE by the Shockley-Queisser limit, but there are new tendencies in order to reach higher PCE [5, 6, 7, 8] as substitutes of Shockley-Queisser models. Among them, it stands out the use of nanostructures solar cell materials [2, 9, 10]. In fact, semiconductor nanowires (NWs) are low–dimensional systems where two dimensions have length scales between a few and hundreds of nanometers yielding a high aspect ratio [11]. Due to these geometrical properties of the NWs, their light interaction features are different than that of bulk material [2]. Therefore, the NWs and NW arrays appear as good candidates for higher-efficiency solar cells [12, 13, 14] with excellent light trapping properties [15]. In addition, the NW solar cells can enhance carrier collection efficiency [16]. Most NW arrays are fabricated with semiconductor materials as c-Si [14, 17], a-Si [15], CdTe [13], GaAs [18, 19] and InAs [20] among others. Indeed, III-V materials have several advantages over other materials because of a much shorter absorption depth and a wide range of variable band gaps [16]. Besides, the III-V NW solar cells present the highest reported PCE [21, 22]. Among the III-V semiconductors, GaAs seems a promising candidate for making NWs solar cells. This is mainly due to its large absorption coefficient and the easiness of fabrication by conventional growth techniques [16].

In this paper, we investigate the optical properties of a vertically oriented square array of GaAs NWs based photovoltaic solar cells, focusing on their reflectance, to gain insight about the system efficiency. A small value of the reflectance in the NWs array will entail a better absorption in the array and consequently, a higher efficiency. For this study, we use the transfer matrix formalism to analyze the optical reflectance using Fresnel reflectivities within the stacked layers. To simulate NWs array with small diameters and periodic structures, transfer matrix method has been proven to be very effective for dealing with periodic structures [23]. To define the dielectric function of the effective medium consisting of NWs and islanding material we use the Maxwell–Garnett model [24], which is appropriate when the filling factor of the effective medium investigated is small enough such as in our system. To describe the dielectric function of the NW, the square arrays are treated as a continuum medium through the use of the Webb formalism [25] for each one of NW, where the exciton confinement energy is considered as resonance frequency. That formalism has proven to be successful for low–dimensional systems such as our NWs. The rest of paper is organized as follows. In section 2, the transfer matrix formalism and Maxwell–Garnett model along with the Webb model are described to calculate the reflectance of square array of GaAs NWs. The implementation of the model in our system along with a discussion of the results are given in section 3. The main remarks and conclusion of this work will be given in section 4.

2. Theoretical model

We investigate the optical properties of a square array of GaAs cylindrical NWs embedded in epoxy, taken as an example of embedding medium. The array is characterized by a cylinder radius $R = 10\ nm$, and length $h = 500\ nm$ and an array´s periodicity or pitch $a = 80\ nm$. These geometrical values yield a filling factor ($f = \pi(R/a)^2$) for the investigated system equal to $f = 0.049$. Figure 1 shows the scheme of cylindrical array, where the parallel and perpendicular directions to the cylinders axis are z- and x- and y-axes, respectively. We also depict the s- and p-polarizations configuration for sake of clarity.

In the following simulations, the values of the above geometrical parameters of the array are maintained constant throughout the computing process to evaluate the optical properties. In addition, for the sake of simplicity, we restrict our simulations to the system where we have not considered the

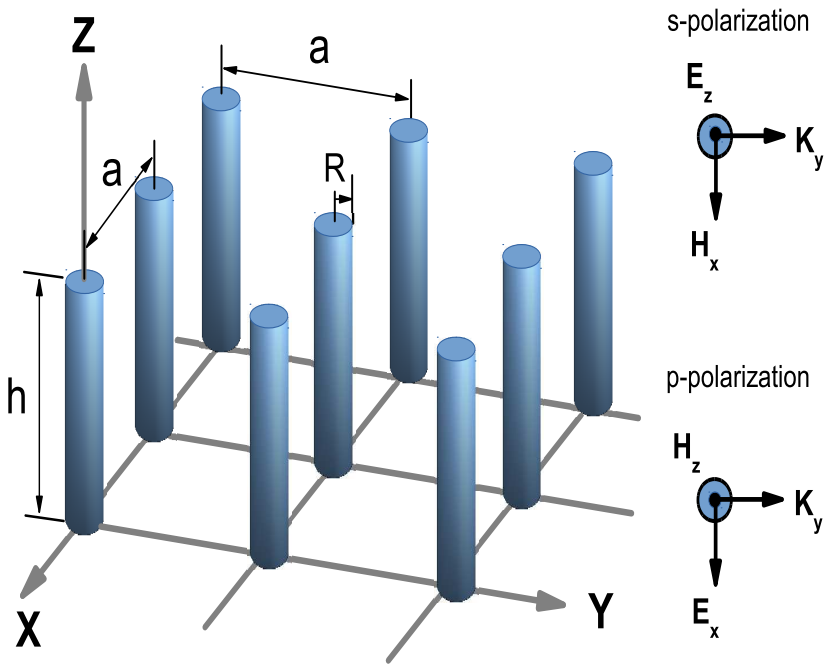

Figure 1: *Scheme of the GaAs NWs array, where z axis is along the NW axis. The array is characterized by periodicity parameter $a = 80$ nm, the length of the NW is $h = 500$ nm and its radius is $R = 10$ nm. The representation of s- and p-polarization is included in the scheme.*

effect of the substrate. The array is then modeled by a multilayer system composed of n periodic bilayers, where each bilayer is constituted by (i) a film of epoxy with dielectric constant $\epsilon_e = 3$ and thickness $b = a/2 = 40$ nm and (ii) a film of GaAs NWs embedded in epoxy with an effective dielectric function, which will be discussed later, and with thickness $b = a/2$ $= 40\ nm$. This bilayer is periodically distributed in the space up to n periods.

To study the effect of periodicity, we consider a sample composed of repetition of n unit cells made up of bilayers in the direction of propagation of the incident light (see Figure 2). Figure 2 depicts the scheme of the multilayer system, where we emphasize on the direction of the incident light. We implement the numerical simulations over the wavelength range which cover the relevant parts of solar spectrum.

The reflection spectrum of the multilayer system is calculated using Fresnel expressions for n periodic bilayers in terms of the transfer matrix [26]. In fact, the characteristic matrix of a bilayer, is given by [27]

$$\mathrm{M}=\frac{1}{1-r_{12}^2}\begin{pmatrix} e^{-i(\phi_1+\phi_2)}-r_{12}^2e^{-i(\phi_1-\phi_2)} & r_{12}(e^{i(\phi_1+\phi_2)}-e^{i(\phi_1-\phi_2)}) \\ r_{12}(e^{-i(\phi_1+\phi_2)}-e^{-i(\phi_1-\phi_2)}) & e^{i(\phi_1+\phi_2)}-r_{12}^2e^{i(\phi_1-\phi_2)} \end{pmatrix} (1)$$

where r_{12} is the reflection coefficient at the 1/2 interface and ϕ_1 and ϕ_2 are the phase differences of layers 1 and 2, respectively (see figure 2). Then, the light getting trough n periodic bilayers will be defined by M^n, where for a high value of n, the transfer matrix M^n has a huge expression. The overall reflection coefficient from the multilayer system is then given by $r = M_{21}/M_{11}$, where M_{21} and M_{11} are the elements of the final transfer matrix (M^n) [28]. This theoretical approach thus allow us to calculate the reflectance for s- and p-polarizations, $R^{(s,p)}$, from the NWs array in form of $R^{(s,p)} = |r^{s,p}|^2$. Herein, the superscripts s and p refer to the s- and p-polarizations, respectively. Then, the expression of coefficient $r^{(s,p)}$ depends of the number of repeated bilayers considered in the study. For higher n, its expression is more complicated; therefore, we only describe the mathematical expression of the reflection coefficient at the 1/2 interface, which appears in eq. (1). This coefficient is essential in the definition of the overall reflection coefficient $r^{s,p}$; i.e.,

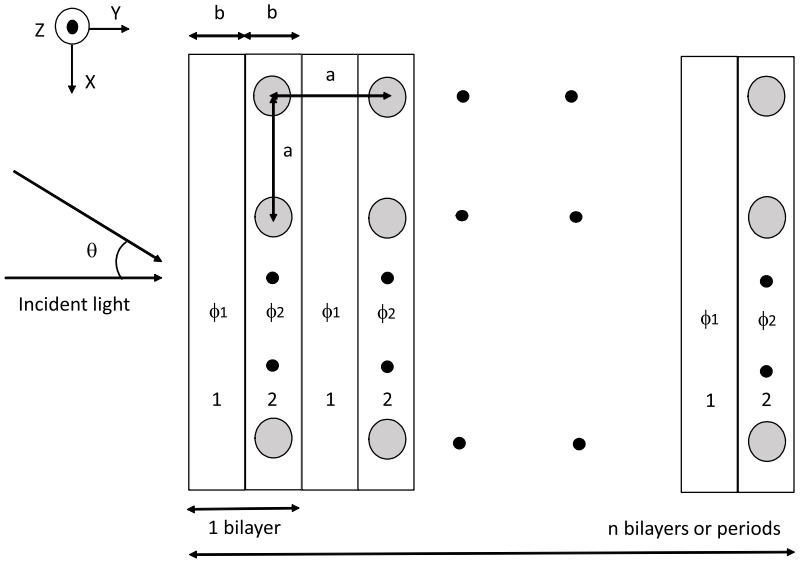

Figure 2: *Scheme of the multilayer system constituted by bilayers of epoxy (film 1) and GaAs NWs embedded in epoxy (film 2) of equal thicknesses, being the phase differences for films 1 and 2, ϕ_1 and ϕ_2, respectively. The multilayer is constituted by n bilayers or periods.*

$$r_{12}^{s} = \frac{k_1^{||}(\omega) - k_2^{||}(\omega)}{k_1^{||}(\omega) + k_2^{||}} \tag{2}$$

for s-polarization and

$$r_{12}^{p} = \frac{\epsilon_1^{||}(\omega)k_2^{\perp}(\omega) - \epsilon_2^{||}(\omega)k_1^{\perp}(\omega)}{\epsilon_1^{||}(\omega)k_2^{\perp}(\omega) + \epsilon_2^{||}(\omega)k_1^{\perp}(\omega)} \tag{3}$$

for p-polarization. In eqs. (2) and (3), the superscripts ($||$) and ($\perp$) refer to the parallel and perpendicular directions to the axis of the cylindrical NWs. The wave vectors and dielectric functions in the above equations are a generalization of those reported in reference [28]; i.e.,

$$k_1^{||}(\omega) = k_1^{\perp}(\omega) = \frac{\omega}{c}\sqrt{\epsilon_1}cos\theta, \tag{4}$$

where layer 1 is epoxy, an isotropic material, with dielectric constant $\epsilon_1 = \epsilon_e = 3$, θ is the angle of incident light (see figure 2) and c the speed of ligth;

$$k_2^{||}(\omega) = \frac{\omega}{c}\sqrt{\epsilon_2^{||}(\omega) - \epsilon_1 sin^2\theta}, \tag{5}$$

and

$$k_2^{\perp}(\omega) = \frac{\omega}{c}\sqrt{\frac{\epsilon_2^{||}(\omega)}{\epsilon_2^{\perp}(\omega)}}\sqrt{\epsilon_2^{\perp}(\omega) - \epsilon_1 sin^2\theta} \tag{6}$$

where layer 2 is an effective medium constituted by GaAs NWs embedded in epoxy, being $\epsilon_2^{||}(\omega)$ and $\epsilon_2^{\perp}(\omega)$ the effective dielectric functions in the directions parallel and perpendicular to the axis of cylindrical NWs. The phase differences ϕ_1 and ϕ_2, appearing in eq. 1 and fig. 2, are defined by $\phi_1 = k_1^{||}.b$ and $\phi_2 = k_2^{||}.b$ or $\phi_2 = k_2^{\perp}.b$ for s- or p-polarization, respectively. When $\theta = 0^o$, $k_2^{||} = k_2^{\perp}$ and consequently, the phase difference ϕ_2 is equal for s- and p-polarization.

For modeling the electromagnetic response of a GaAs NWs array, we use the Maxwell-Garnett model with the Clausius–Mossotti correction as it is based on a rigurous solution of Maxwell equations under the assumption of a small inclusion density [24, 29]. Therefore, the effective permittivity of one layer constituted by GaAs NWs embedded in epoxy in the direction parallel to the cylinder axis, denoted by $\epsilon_2^{||}(\omega)$, can be written as [29]

$$\epsilon_2^{||}(\omega) = \epsilon_e \left(1 + f\alpha^{||}(\omega)\right) \tag{7}$$

where f is the filling factor equal to 0.049 and $\alpha^{||}(\omega)$ is given by

$$\alpha^{||}(\omega) = \frac{\epsilon_{nw}(\omega) - \epsilon_e}{\epsilon_e} \tag{8}$$

being $\epsilon_{nw}(\omega)$ the GaAs NW dielectric function that we will describe later. On the other hand, the permittivity of the effective medium in the direction perpendicular to the cylinder axis, denoted by $\epsilon_2^{\perp}(\omega)$, can be written as [29]

$$\epsilon_2^{\perp}(\omega) = \epsilon_e \left(1 + \frac{f\alpha^{\perp}(\omega)}{1 + 0.5f\alpha^{\perp}(\omega)}\right) \tag{9}$$

where

$$\alpha^{\perp}(\omega) = \left(\frac{\epsilon_e}{\epsilon_{nw}(\omega) - \epsilon_e} + 0.5\right)^{-1}. \tag{10}$$

Finally, we will describe the dielectric function of GaAs NWs. Due to NWs are low–dimensional systems as quantum dots, we follow the same formalism used by Webb et al.[25] to define the GaAs NWs dielectric function; i.e.,

$$\epsilon_{nw}(\omega) = \epsilon_\infty + \frac{8e^2}{V\epsilon_o m_{ex}} \left[\frac{2\rho - 1}{\omega_{ex}^2 - \omega^2 - i2\omega\gamma}\right] \tag{11}$$

being ϵ_∞ the GaAs dielectric constant at high frequency, e the electron charge, ϵ_o the vacuum permittivity and m_{ex} the exciton reduced mass for GaAs. As the hole effective mass, m_h^*, is greater than the electron effective mass, m_e^*, then $1/m_{ex} = 1/m_e^* + 1/m_h^* \approx 1/m_e^*$; V is the volume of the cylindrical NW, $\rho = 1$ for lossy resonance, ω_{ex} the exciton frequency and γ a dumping constant equal to 27.1 cm^{-1} [30]. For a cylindrical potential well with infinite barriers at $r = R$, we assume the approximate exciton energy ($E_{ex} = h\omega_{ex}$)

$$E_{ex} = E_g + \frac{\hbar^2\chi_{0,1}^2}{2m_e^*R^2} + \frac{\hbar^2\pi^2}{2m_e^*d^2} \tag{12}$$

where $E_g = 1.424\ eV$ ($= 870\ nm$) is the intrinsic GaAs band gap energy and the second and third terms describe the kinetic energy of the exciton in the perpendicular and parallel directions to the NW axis, respectively. For this

definition, we consider the extreme quantum limit, where only the fundamental level is occupied. Then, $\chi_{0,1}$ is the first zero of the cylindrical Bessel function and the third term of the above equation represents the fundamental energy of an infinite square well of width $d = 2\ R$. As the GaAs NWs are embedded in the islanding material epoxy, our approach seems appropriately justified. On the other hand, the formalism used in eq. (12) to define the exciton energy is a specific case to that reported for excitons energy in spherical quantum dots [25], where we have not taken into account the exciton Coulomb interaction term due to its contribution is small compared with the kinetic terms [31].

3. Results and discussion

The simulated GaAs NWs array -multilayer system- and its structural parameters have been schematically described in figures 1 and 2. The reflectance of this structure is discussed in terms of the transfer matrix for a number of periodic bilayers n. For the sake of simulation simplicity, we will take until nine bilayers, because this number is large enough to obtain the main features of the array reflectance. Indeed, $n = 9$ bilayers is equivalent to 18 single alternated GaAs NW -epoxy layers, that is enough to converge to acceptable result. On the other hand, the effective medium consisting of GaAs NWs embedded in epoxy is described with an extended Maxwell–Garnett model. As the investigated system has cylindrical symmetry, we will define its effective dielectric function in the directions perpendicular and parallel to the NW axis. Also, to clarify the presentation of our results, we divide our discussion in two subsections, accounting for the system reflectance for s- and p-polarized light.

3.1. GaAs NWs reflectance for s-polarized light

The s-polarized light (TE) occurs when the electric field of the electromagnetic wave is perpendicular to the incidence plane [27]. From our scheme of figure 1, the electric field is along the z-axis for this polarization. We show in figure 3 the reflectance of the system for incident angle $\theta = 0^{\text{o}}$ and for a number of bilayers equal to 3, 5, 7 and 9. As it can be seen in figure 3, the oscillating behavior of the reflectance is almost similar for all number of bilayers. In fact, this behavior is more significant for wavelength below 300 nm, where the number of oscillations is increasing and the last oscillation is

red-shifted with the number of bilayers. The oscillating behavior is consistent with the periodicity of the system. We expect that for a critical number of bilayers, the light does not cross through the entire array. Then, this process would explain the broadening and red-shift of the last oscillation in the reflectance spectra for increasing number of bilayers. Also, an increasing number of bilayers for a fixed angle of incident light, entails a higher number of scattering centers between the electric field and the NWs, giving a higher number of oscillations and consequently, smaller distance between oscillation maxima. We obtain an approximate law for the distance between maxima as (5.5 - 0.5 n), where n is the number of bilayers.

The effects of interference in periodical systems yield oscillations in their reflectance [20]. As white light impinges on the NWs, photons can interact with NWs and undergo multiple scattering, yielding interference effects due to relative phase difference between reflected waves. In fact, this behavior is also reported for the reflectance of other periodical systems like porous Si NWs [32], III-V NWs [16, 33, 34], metamaterials [35] and carbon nanotubes [36]. In addition, the oscillating behavior of absorbance and transmittance of nanorods and NWs solar cells is reported elsewhere [23, 37, 38, 39]. Also, we find in the reflectance spectra a feature peaked around 850 nm which can be ascribed to the band gap of GaAs. Sanatinia et al. [40] obtained a similar feature around 850 nm in the total reflectance spectra of frustrum GaAs nanopillar array. Some authors claim that the absorption of the NWs array strongly depends on the D/a ratio and NW diameter [41, 42]. Figure 4 shows the reflectance of the system for incident angle $\theta = 0^{o}$, 9 bilayers and different ratio D/a, where D is the diameter of the NWs. We obtain that below a critical ratio, the feature at 850 nm tends to disappear. In our case, this critical value is around 0.13 (see figure 4).
Since the transfer matrix has a huge expression for increasing number of periods and consequently, the calculation time is greater, it is necessary to adopt a compromise between number of investigated bilayers and calculation time. For this study of s-polarization, we adopt 9 bilayers, where in figure 3, we showed that all oscillations lie under the same enveloping curve (dashed curve as a guideline for the eyes). Therefore, our simulations can supply an upper limit of the reflectance values for a greater number of bilayers; then, the increase of bilayers in the calculation does not give extra information on the array reflectance.

We also investigate the reflectance dependence on the light incidence angle. Figure 5 shows the reflectance for $\theta = 0^{o}$, 30^{o}, 45^{o} and 60^{o} and 9

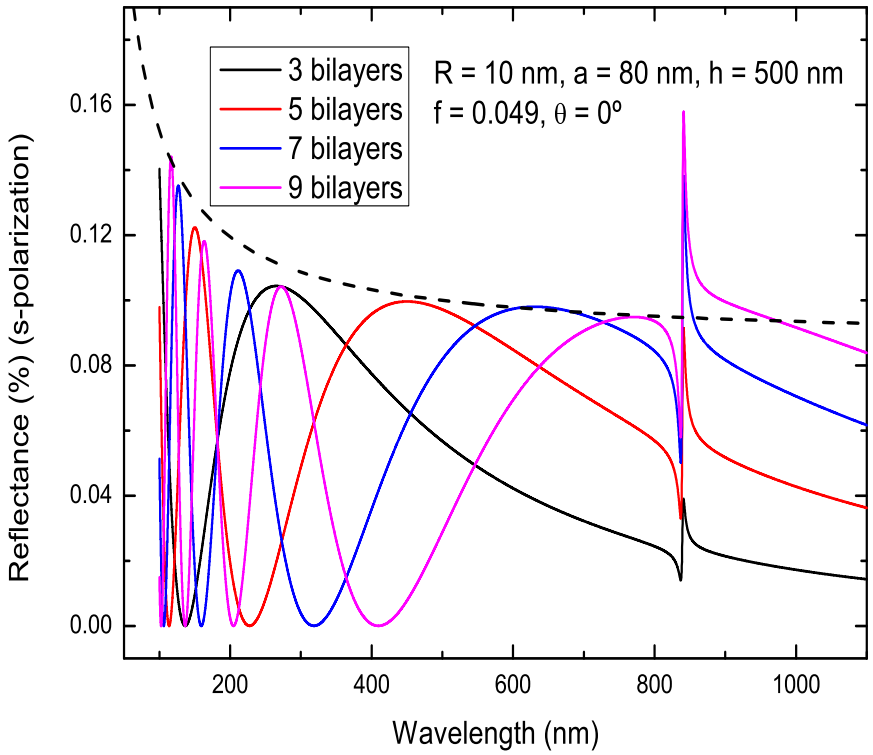

Figure 3: *Reflectance for s-polarized light of the GaAs NWs array for 3, 5, 7 and 9 periods and angle of incidence $\theta = 0^o$. The dashed curve is a guideline for the eyes.*

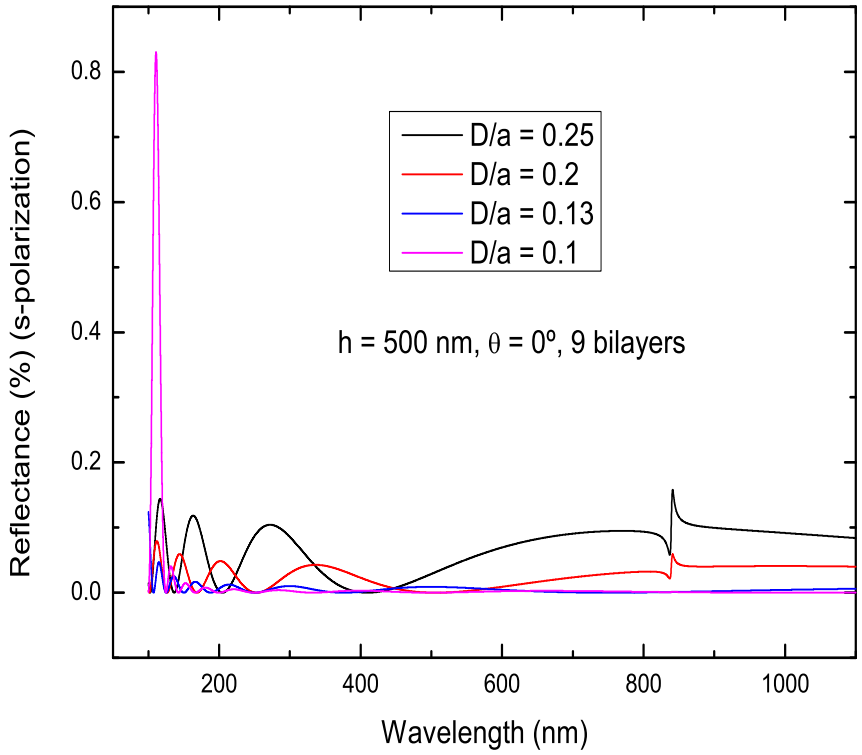

Figure 4: *Reflectance for s-polarized light of the GaAs NWs array for 9 bilayers, angle of incidence $\theta = 0^o$ and different ratios D/a.*

bilayers. Our simulations prove that for increasing angle, the intensity of the reflectance is higher for s-polarized light, similar to that reported for s-polarized reflectance of InAs NWs [20] and metamaterials [43]. By increasing the incidence angle, for a fixed number of bilayers, the electric field detects less number of scattering centers, then the number of oscillations decreases and consequently, the distance between oscillation maxima increases [20]. We obtain an approximate law for the distance between maxima as $(0.99 + 0.02\ \theta + 5.5\ \times 10^{-4}\theta^2)$, where θ is the incident angle. A small value in the reflectance would imply a better absorption of incident light, improving the efficiency of photovoltaic solar cells. Then, to obtain a better efficiency of the photovoltaic solar cells, the angle of the incident light should be 0^o for s-polarized case. In addition, we evaluated the reflectance for 60^o with 3, 5, 7 and 9 bilayers (not shown here) and we found that the oscillations lie under an enveloping curve, proving that the election of 9 bilayers is good enough, as we discussed above.

3.2. GaAs NWs reflectance for p-polarized light

The p-polarized light (TM) occurs when the electric field of the electromagnetic wave is parallel to the incidence plane [27]. From our scheme of figure 1, the electric field is along the x-axis for this polarization. We show in figure 6 the reflectance of the system for incident angle $\theta = 0^o$ and for 3, 5, 7 and 9 bilayers.

We obtain an oscillating behavior of the reflectance, exactly similar to that obtained for s-polarization (see figure 3). In fact, Sikdar and Kornyshev [28] have shown that so far the normal incidence is considered, reflectance spectra undergo identical reflection both for s- and p-polarized light for nanoparticle layers. The similarity of our simulations between s- and p-polarization at $\theta = 0^o$ is characterized by the same: (i) intensity, (ii) dependence of reflectance with the number of bilayers and (iii) feature peaked at 850 nm. As we commented in section 2, when $\theta = 0^o$, $k_2^{||} = k_2^{\perp}$ and consequently, the phase difference ϕ_2 is equal for s- and p-polarization. Then, we can deduce that the phase difference is more relevant than the reflection coefficient at the 1/2 interface, r_{12}, in the evaluation of the transfer matrix (see eq. 1). In addition, the election of up to 9 bilayers gives a reasonable approximation to calculate the reflectance for p-polarization, such as we discussed above for s-polarization. These simulations can also supply an upper limit of the reflectance values for a greater number of bilayers (see dashed curve in figure 6).

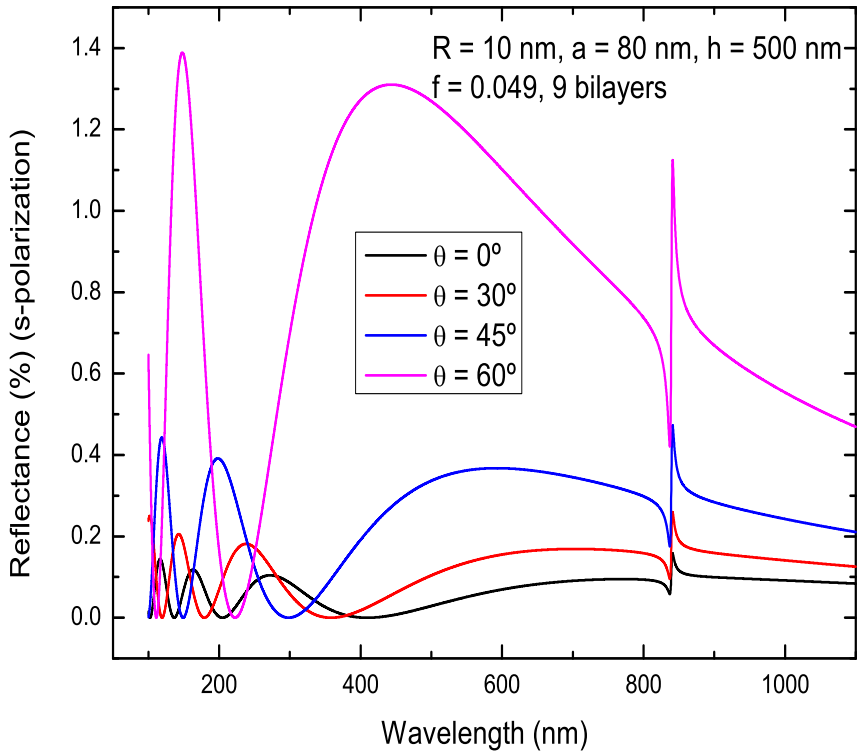

Figure 5: *Reflectance for s-polarized light of the GaAs NWs array for 9 bilayers and angles of incidence $\theta = 0^o$, 30^o, 45^o and 60^o.*

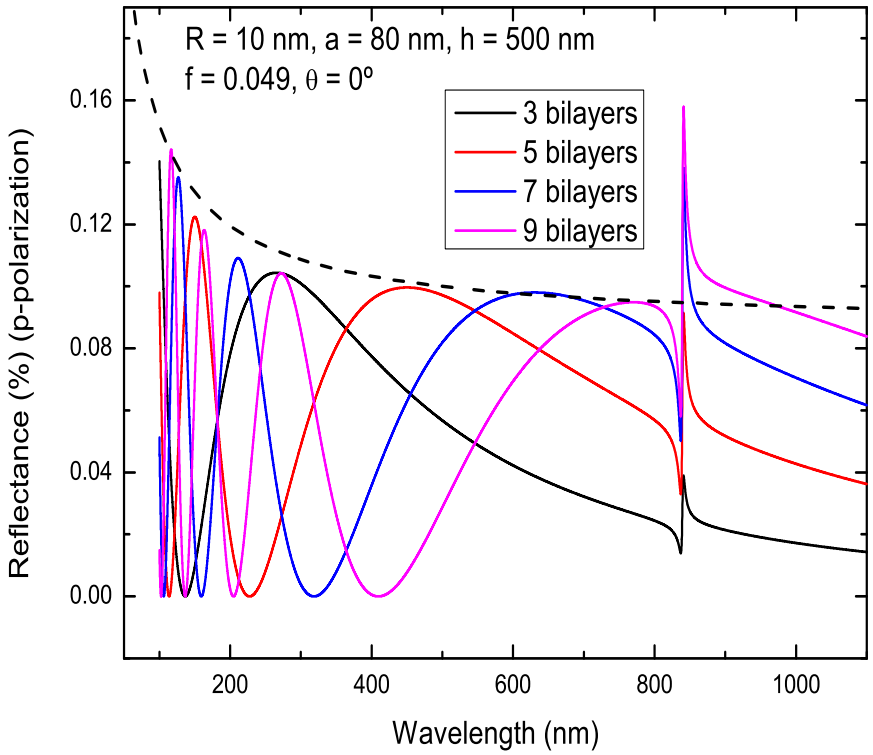

Figure 6: *Reflectance for p-polarized light of the GaAs NWs array for 3, 5, 7 and 9 bilayers being the angle of incidence $\theta = 0^o$. The dashed curve is a guideline for the eyes.*

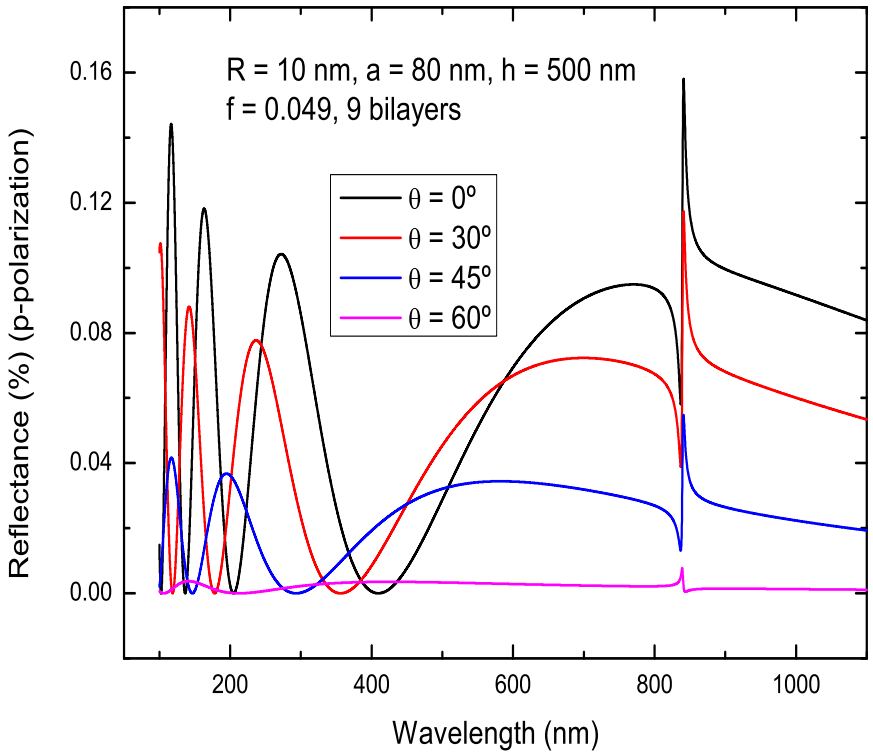

Figure 7: *Reflectance for p-polarized light of the GaAs NWs array for 9 bilayers with angles of incidence $\theta = 0^o$, 30^o, 45^o and 60^o.*

We also investigate the reflectance dependence on the light incidence angle. Figure 7 shows the reflectance for $\theta = 0^o$, 30^o, 45^o and 60^o and for 9 bilayers. Our simulations show that for increasing angle, the intensity of the reflectance is smaller, conversely to the case for s-polarized light. This behavior is equivalent to that reported for p-polarized reflectance in InAs NWs [20] and metamaterials [43]. For $\theta = 60^o$, we obtain quasi-zero reflectance values and an anomalous behavior for the peak at 850 nm. Then, for higher incident angles, we expect an evanescent feature of the p-polarized reflectance. Besides, the reflectance values obtained for p-polarization is 10 times lower than that of s-polarization when the incident angle is great (see figures 5 and 7). Therefore, to gain efficiency of the photovoltaic solar cells, the p-polarization is better than the s-polarization for high incident angles.

4. Conclusion

We have calculated the optical reflectance of GaAs NWs array based on transfer matrix formalism and Maxwell–Garnett model. Simulations are performed for s- and p-polarized light. The election of up to 9 bilayers gives a reasonable approximation to simulate the reflectance spectra. An oscillating behavior of the reflectance is found for both cases, similar to that reported in the literature for porous silicon and III-V semiconductor NWs. We have also obtained a feature peaked around 850 nm, characteristic of the GaAs band gap. Attending to the reflectance dependence on the incident angle, we have found that for s-polarized light, the reflectance is higher for increasing angles, conversely to the case of p-polarized light. In fact, the reflectance for p-polarization is 10 times lower than that of s-polarization for high incident angles. Therefore, to obtain good efficiency, it is suitable to use non–zero incidence in p-polarization where the reflectance intensity is seen to be better that of s-polarization. However, in normal incidence, both s- and p-polarization are equivalent. From the above successful results, which combine quantum and effective dielectric theories, we focus in a future work on the influence of the geometrical parameters (radius, length and pitch) of the array along with the composition (band gap energy) on the reflectance of the III-V semiconductors. These parameters could be relevant in the evaluation of absorption and efficiency in semiconductor NWs based solar cells. Finally, we propose that our numerical results could insight light for later reflectance measurements in semiconductor NWs array. In fact, an estimation of the

bilayers number versus the oscillations number is obtained. Also, this study can determinate optimum angles to gain efficiency in semiconductor NWs based solar cells.

CRedit authorship contribution statment

R.M. de la Cruz: Conceptualization, Investigation, Software, Writing-original draft. **C. Kanyinda-Malu:** Investigation, Writing-review.
J.E. Muñoz Santiuste: Funding acquisition, Investigation, Writing-review.

Funding sources

This work is partially supported by Spanish MICINN under grant RTI 2018-101020-B-I00 and TECHNOFUSION III CM–S2018IEMAT–4437. This work has also been supported by Comunidad de Madrid (Spain)-multiannual agreement with UC3M (Excelencia para el Profesorado Universitario-EPUC3M14)-Fifth regional research plan 2016-2020.

References

[1] S. Chu and A. Majumdar, Nature **488** (2012) 294.

[2] G. Otnes and T. Borgström, Nano Today **12** (2017) 31.

[3] A. Polman, M. Knight, E.C. Garnett, B. Ehrler and W.C. Sinke, Science **352** (2016), http://dx.doi.org/10.1126/science.add4424.

[4] N.S. Lewis, Science **351** (2016) 4868, http://dx.doi.org/10.1126/science.aad1920.

[5] M.A. Green, Third Generation Photovoltaics, Springer, New York, 2006.

[6] G. Conibeer, Mater. Today **10** (2007) 42.

[7] D. Ginley, R. Collins and M. Green, MRS Bull. **33** (2008) 355.

[8] A. Polman and H.A. Atwater, Nat. Mater. **11** (2012) 174.

[9] L. Tsakalakos, Mater. Sci. Eng. R: Rep. **62** (2008) 175.

[10] M.C. Beard, J.M. Luther and A.J. Nozik, Nat. Nanotechnol. **9** (2014) 951.

[11] N.P. Dasgupta, J. Sun, C. Liu, S. Brittman, S.C. Andrews, J. Lim, H. Gao, R. Yan and P. Yang, Adv. Mater. **26** (2014) 2137.

[12] B. Kayes, H. Atwater and N.S. Lewis, J. Appl. Phys. **97** (2005) 114302.

[13] Z. Fan, D.J. Ruebusch, A.A. Rathore, R. Kapadia, O. Ergen, P.W. Leu and A. Javey, Nano Res. **2** (2009) 829.

[14] E. Garnett and P. Yang, Nano Lett. **10** (2010) 1082.

[15] J. Zhu et al., Nano Lett., Article ASAP (2009).

[16] A. Gu, Y. Huo, S. Hu. . Sarmiento, E. Picket, D. Liang, S. Li, A. Liu, S. Thombare, Z. Yu, S. Fan, P. McIntyre, Y. Cui and J. Harris, IEEE 978-1-4244-5892-9 (002034) (2010).

[17] M.D. Kelzenberg et al., Nature Materials **9** (2010) 239.

[18] J. Czaban, D.A. Thompson and R.R. LaPierre, Nano Lett. **9** (2009) 148.

[19] C. Colombo et al., Appl. Phys. Lett. **94** (2009) 94.

[20] F. Floris, L. Fornasari, A. Marini, V. Bellani, F. Banfi, S. Roddaro, D. Ercolani, M. Rocci, F. Beltram, M. Cecchini, L. Sorba and F. Rossella, Nanomaterials **7** (2017) 400; doi:10.3390/nano7110400.

[21] J. Wallentin, N. Anttu, D. Asoli, M. Huffman, I. Aberg, M.H. Magnusson, G. Siefer, P. Fuss-Lailuweir, F. Dimroth, B. Witzigmann, H.Q. Xu, L. Samuelson, K. Deppert and M.T. Borgström, Science **339** (2013) 1057.

[22] L. Aberg, G. Vescovi, D. Asoli, M.T. Björk and L. Samuelson, IEEE J. Photovolt. **6** (2016) 185.

[23] N.M. Ali and N.H. Rafat, Renewable and Sustainable Energy Reviews **68** (2017) 212 and references herein.

[24] J.C. Maxwell Garnett, Trans. of the Royal Society, (1904) v. CCIII 385.

[25] K.J. Webb and A. Ludwig, Phys. Rev. B **78** (2008) 153303.

[26] M. Born et al., Principles of Optics, doi: 10.1017/CBO9781139644181 (Cambridge University Press, 1999).

[27] J.M. Cabrera, F. Agulló and F.J. López, Optica electromagnética, Vol. II: Materiales y aplicaciones, Addison Wesley Iberoamericana Española 2000.

[28] D.Sikdar and A.A. Kornyshev, Scientific Reports 33712, doi:10.1038/srep33712(2016) www.nature.com/scientificreports.

[29] G.Y. Slepyan, S.A. Maksimenko, V.P. Kalosha, J. Herrmann, N.N. Ledentsov, I.L. Krestnikov, Z.I. Alferoz and D. Bimberg, Phys. Rev. B **19** (1999) 12275.

[30] A.G.Rolo, L.G.Vieira, M.J.M.Gomes, J.L.Ribeiro, M.S.Belsley and M.P.dos Santos, Thin Solid Films **312** (1998) 348.

[31] R.M. de la Cruz and C. Kanyinda-Malu, Physica E **44** (2012) 1250.

[32] A. Najar, J. Charrier, P. Pirasteh and R. Sougrat, Optics Express **20** (2012) 16861.

[33] Y. Chen, O. Höhn, N. Tucher, M.-E. Pistol and N. Anttu, Optics Express **25** (2017) 294641.

[34] S.L. Diedenhofen, O.T.A. Janssen, G. Grzela, E.P.A.M. Bakkers and J. Gómez Rivas, ACS Nano **5** (2011) 2316.

[35] T.U. Tumkur, J.K. Tikur, B. Chu, L. Gus and V.A. Podolskiy (2012), Birch and NCN Publications Paper 1146, http://dx.doi.org/10.1063/1.4746387.

[36] H. Bao, X. Ruan and T.S. Fisher, Optics Express **18** (2010) 6347.

[37] E.C. Garnett, M.L. Brongersma, Y. Cui and M.D. McGehee, Annu. Rev. Mater. Res. **41** (2011) 269.

[38] G. Mariani, A.C. Scofield, C.-H. Hung and D.L. Huffaker, Nature Communications, doi: 10.1038/ncomms2509 (2013).

[39] Y. Chen, M.-E. Pistol and N. Anttu, Scientific Reports (2016) doi: 10.1038/srep32349.